Frequency Control Services from Scaled-up Hydrogen Electrolysis Plants Considering Power Dispatch Strategies

Ridma Wijethunga
Monash University
Melbourne, Australia
ridma.wijethunga@monash.edu

Behrooz Bahrani
Monash University
Melbourne, Australia
behrooz.bahrani@monash.edu

Mehdi Ghazavi Dozein
Monash University
Melbourne, Australia
mehdi.ghazavidozein@monash.edu

***Abstract*—This paper examines the frequency support capability of hydrogen electrolysis plants, considering multiple stacks scaled-up together under different dispatch strategies. We propose a dynamic model of a multi-stack electrolysis plant where a common grid-side converter is used for all stacks, each of which is interfaced through an individual DC–DC converter. The plant control includes a power dispatch unit responsible for allocating available power across the stacks. The model further represents essential electrolyzer operational constraints, including ramp rate and partial load limits. Our study clarifies how different power dispatch strategies (e.g., average allocation, daisy-chain allocation) and operational constraints interact and may impact the available headroom/footroom for frequency control services, the associated response time, and the aggregate equivalent plant operational limitations. The simulation results indicate that the average allocation strategy reduces the available footroom for upward frequency control services and improves the plant ramp rate. Conversely, the daisy-chain allocation strategy tends to offer a larger room for power reduction during under-frequency events, though at the expense of more restrictive ramp rate performance. The findings of this study should be considered by system operators and project developers when planning system support services from large-scale electrolysis plants.**

***Index Terms*—Frequency control, Partial load limit, Power dispatch strategies, Ramp rate limit, Scale-up requirements, Scaled-up hydrogen electrolyzers.**

I. Introduction

The rapid growth of inverter-based technologies, such as renewable energy sources (RES), has reduced synchronous inertia and tightened frequency stability margins in power systems around the world [1], [2]. While there are few technological solutions available to support system stability such as battery storage systems, there is a potential in providing frequency control services from large inverter-based loads (IBLs) such as hydrogen electrolyzers (HEs). Electrolyzers can change their active power consumption over sub-second to multi-second timeframes, thus being able to mitigate active power mismatch and frequency excursions [3]. There are currently trial projects underway to demonstrate the flexible operation of electrolysis technologies for system frequency services, such as the 10 MW electrolyzer in Germany's REFHYNE project [4], 100 MW electrolyzer in the United Kingdom's Gigastack project [5], and 10 MW electrolyzer in Japan's FH2R project [6], among others.

While the existing literature generally analyzes HE frequency control capability using only a single electrolysis stack, practical large-scale electrolysis facilities comprise multiple stacks that are scaled up and coordinated through a specific dispatch strategy [7]. For example, the references [1], [8] propose dynamic models for large-scale HEs providing frequency control services. However, the entire HE system is modeled as a single unit with one stack and the associated controls. Ignoring the scaled-up plan and requirements, electrolysis plant dispatch strategy, and operational limits produces an inaccurate picture of electrolyzer capabilities in system frequency services. In [9], the authors propose a dynamic power allocation control strategy for hybrid hydrogen systems providing frequency control, with no discussions on power dispatch strategy and its impacts on the available range for service provision. Similarly, the impacts of dispatch strategy on both the available range for frequency control provision and the HE response time is not investigated in [10] and [11].

In [12]–[14], two main categories of power dispatch strategies have been identified for multi-stack HE plants: the average allocation (AVA) strategy and the daisy-chain allocation (DCA) strategy. In AVA, the available power is allocated equally among all stacks, while in DCA stacks are activated sequentially once the preceding stack reaches its predefined power threshold. Based on these two strategies, previous research works attempted to optimize power allocation in multiple-stack units in terms of overall efficiency, and limited electrolyzer degradation and uneven stack utilization. However, it is not yet investigated how and to what extent these power allocation strategies may impact the available active power headroom/footroom for HEs, as well as their associated response time, when it comes to frequency control services. It is also not clear how to integrate power dispatch strategy model into the whole HE plant dynamic model with several hydrogen/power controllers and operational limitations. Although partial load and ramp rate constraints are generally defined for individual stacks, the resulting aggregate limitations of a multi-stack HE plant may vary with the chosen

979-8-3315-8138-1

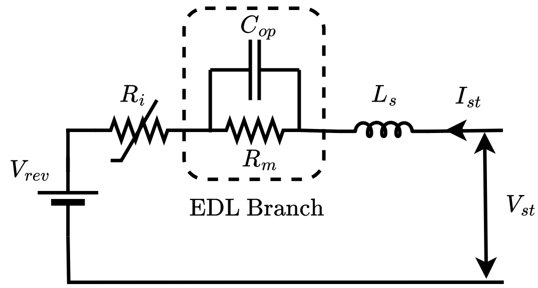

Fig. 1. A generic electrolysis stack model.

dispatch strategy. This is an issue that remains unexplored.

In summary, the contributions of the paper are summarized, as follows:

1) Presenting a detailed dynamic model of a scaled-up HE plant with multiple stack units, coordinated with different power dispatch strategies, connected to the external grid through a power-electronics interface while considering scale-up requirements;
2) Studying the potential impacts of the HE dispatch strategy on its available technical range and response time when providing frequency control services;
3) Highlighting the potential impacts of multi-stack plant dispatch strategy on the aggregate equivalent plant partial load and ramp rate limits.

The rest of the paper is organized, as follows: In Section II, a novel dynamic model for scaled-up HE plants is proposed, which includes HE stack model, power dispatch controller, partial load limiter, and ramp rate limiter. Section III presents the simulation test system, case studies, and discussions. Concluding remarks are presented in Section IV.

II. Proposed Dynamic Model for a Multi-stack HE Plant Considering its Power Dispatch Strategy

A. Electrolysis Stack Model

The fundamental component in the HE plant modeling is the electrolysis stack model. As illustrated in Fig. 1, the electrolysis stack model includes a constant voltage source (V_{rev}), which represents the stack reversible voltage and other components to denote several overpotentials, which are a function of stack current (I), temperature (T), and pressure (P). The internal resistance (R_i) captures stack voltage-current relationship and an Electrical Double Layer (EDL) branch composed of an overpotential capacitor (C_{op}) in parallel with a mass transport resistance (R_m) [1].

In alkaline (ALK) electrolyzer modeling, the inductor L_s should be considered to account for its slow dynamics. It is to note that $L_s \approx 0$ in the case of proton exchange membrane (PEM) electrolyzers because of their inherent fast dynamics. The effect of the EDL branch can be neglected in PEM stacks, while it has a significant effect on ALK stack dynamic behavior [8].

B. Proposed Dynamic Model for Scaled-up HE Plants

Utilizing the stack model presented earlier, a detailed dynamic model of a scaled-up HE plant with multiple stacks is proposed and demonstrated in Fig. 2. The following points are to be noted regarding the proposed dynamic model:

1) AC-DC Converter Controls: In the proposed model, all stacks share a common AC–DC grid-side converter. The converter capacity (P_{GSC}) should be enough to supply all stacks at their rated power (i.e., $P_{GSC} \geq N \cdot P_{rated}$), where N is the number of electrolysis stacks in the hydrogen plant, and P_{rated} is the individual stack rated power. The grid-side AC–DC converter regulates the DC-link voltage and manages the reactive power exchange with the grid. The HE plant is synchronized with the external grid through a phase-locked loop (PLL) unit. The active (P_{ref}) and reactive (Q_{ref}) power references for the converter are generated by the DC-link voltage controller and the Q–V controller, respectively. Given a mismatch between the DC-link voltage (V_{dc}) and its reference (V_{dc}^{ref}), the DC-link controller determines the (P_{ref}) value, while the Q–V controller adjusts Q_{ref} according to the terminal voltage (V_{pcc}) value at the point of common coupling (PCC), according to the Q–V droop characteristic embedded in the HE plant. A pulse-width modulation (PWM) strategy generates the gating signals for the IGBT switches of the grid-side converter. A detailed description of this control scheme can be found in [15].

2) Power Dispatch Control Unit: The power dispatch unit, as per Fig. 2, includes an active power-frequency characteristic to enable HE frequency control provision and calculate the HE power reference (P_{plant}^{ref}), as well as the power dispatch strategy to calculate the power reference for each stack. In the case of frequency disturbances, the frequency deviation (ΔF) is obtained as the difference between the measured grid frequency and the nominal frequency. Then, the calculated P_{plant}^{ref} passes through the power dispatch unit. The power being allocated to stacks depends on the dispatch strategy. In the case of AVA strategy, the available power from the grid is allocated equally to each stack, and the reference power of each stack ($P_{HE,i}^{ref}$) can be calculated from the following equation:

$$P_{HE,i}^{ref} = \frac{P_{plant}^{ref}}{N}, \ (i = 1, 2, ...N). \tag{1}$$

So, all stacks are always in operation together at the same power. In the case of DCA strategy, stacks start to operate one by one. To turn on the next stack, the previous stack must reach its predefined power value (P_{def}) (e.g., 80% of the nominal stack power capacity) [14]. Assuming no partial load limitation on stacks, the $P_{HE_i}^{ref}$ in the DCA strategy can be formulated as:

$$P_{HE_i}^{ref} = \begin{cases} P_{plant}^{ref}, & i = 1, \\ K_i(P_{HE,(i-1)}^{ref} - P_{HE,(i-1)}), & i = 2, .., N, \end{cases} \tag{2}$$

where $K_i = 1$ if $P_{HE,(i-1)} \geq P_{def}$ and $K_i = 0$ otherwise. $P_{HE,i}$ is the active power of the i^{th} stack ($P_{HE,i} =$

979-8-3315-8138-1

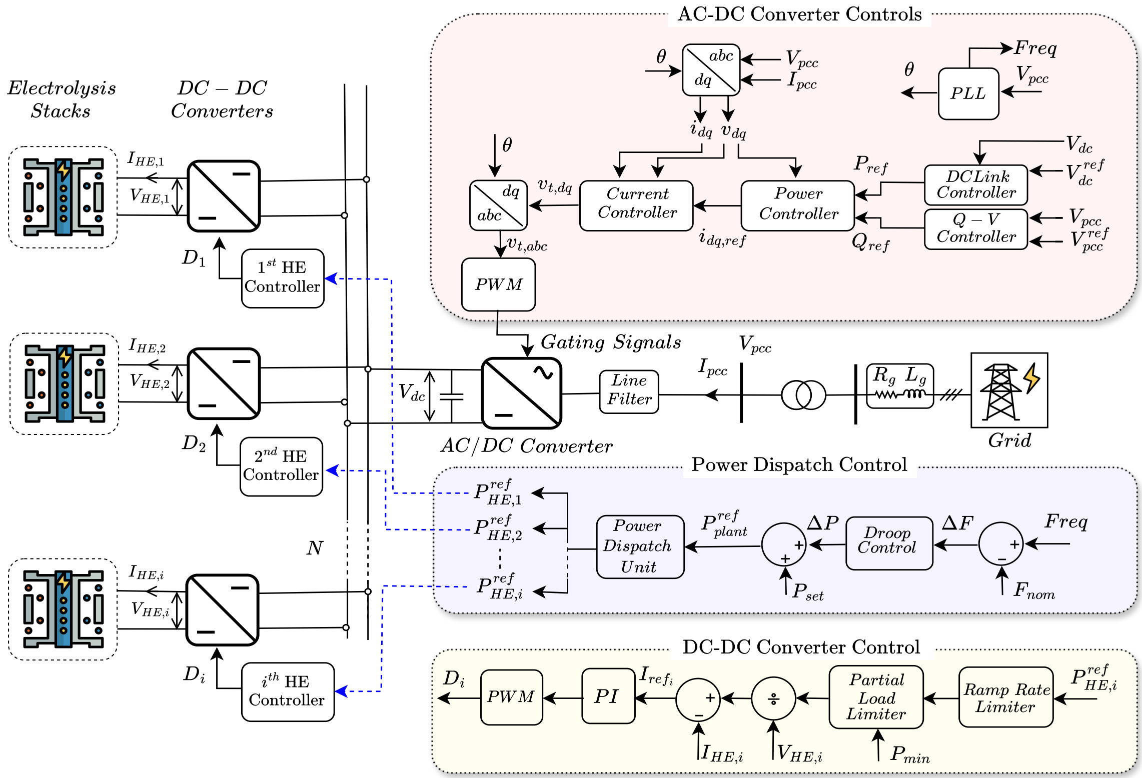

Fig. 2. Proposed scaled-up HE plant dynamic model with power dispatch control unit, partial load limiter, and ramp rate limiter.

$V_{HE,i} \cdot I_{HE,i}$), where V_{HE_i} and I_{HE_i} are the voltage and current of the i^{th} stack, respectively. In the DCA strategy, it is assumed that there is no communication delay and that sequence rotation is implemented to ensure that no single electrolyzer is operated significantly more than the others.

3) DC-DC Converter Control and Operational Limitations: In the proposed model, a DC-DC converter controller regulates the active power of each stack according to the active power reference assigned by the power dispatch control unit. The ramp rate limiter is responsible for maintaining the rate of change of active power within an allowable range during power transient [16]. So, the ramp rate limiter can override the dispatch control unit if the power change rate is beyond the permissible ramp rate. Also, the reference power passes through a partial load limiter, which enforces the stack safe power consumption window. If the reference power falls below the P_{min} threshold, the partial load limiter overrides the dispatch control unit and sets the power to P_{min}, thus all online stacks operating at partial load [17]. Finally, using the stack voltage and current measurements, the PWM technique generates the gating signals for each DC-DC converter.

III. Case Studies

A. Case Study Description

To investigate the efficacy of the proposed multi-stack HE plant model, a PEM HE of 50 MW, with 10 identical stacks rated at 5 MW, is simulated in an electromagnetic transient (EMT) simulation platform. The plant is connected to the external grid, modeled by a Thevenin equivalent with a series impedance (R_g, L_g), as shown in Fig. 2. The parameters used in this simulation study can be found in Table I.

TABLE I
THE PARAMETERS USED IN THE SCALED-UP ELECTROLYSIS PLANT DYNAMIC MODEL.

Parameter	Value
Upstream AC grid voltage	132 kV
Grid inductance (L_g)	100 μH
Grid resistance (R_g)	1 mΩ
Transformer rated voltage	132/11 kV
Line filter inductance (L_f)	38.51 μH
Line filter resistance (R_f)	7.26 mΩ
DC link capacitance (C_{dc})	0.05 F
DC link reference voltage (V_{dc}^*)	18 kV
P-f droop gain (D_p)	23 MW/Hz
Frequency dead-band	0.05 Hz
Stack rated power (P_{rated})	5 MW
Number of stacks (N)	10
Predefined active power threshold (P_{def})	5 MW
Stack reversible voltage (V_{rev})	336 V
Internal resistance (R_i)	0.112 Ω
Mass transport resistance (R_m)	0.02Ω

979-8-3315-8138-1

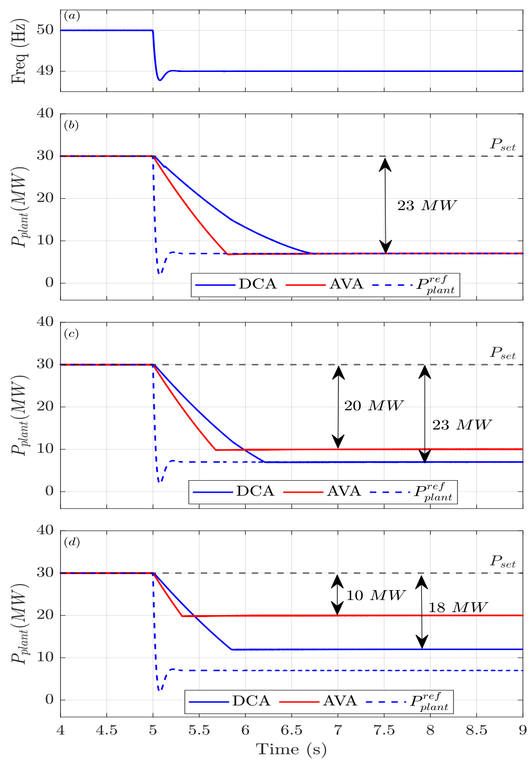

Fig. 3. Power dispatch strategy impacts on HE frequency response volume and the whole-plant partial load limit: (a) Frequency disturbance at t=5 seconds, (b) First scenario results with P_{min} = 0 MW, (c) Second scenario results with P_{min} = 1 MW, and (d) Third scenario results with P_{min} = 2 MW.

The following cases are studied: *Case I* examines how a particular dispatch strategy may impact the available technical range for HE service provision, and the partial load limit of the whole HE plant. *Case II* investigates the aggregate ramp rate limitation of a multi-stack HE plant under a given dispatch strategy, and compares it with the individual stack ramp rate limit, highlighting the importance of accounting for scale-up effects on response time when assessing the actual capabilities of electrolysis plants in service provision.

B. Case I: Dispatch Strategy Impacts on the Whole-plant Partial Load Limit and the Scaled-up HE Frequency Control Services

In *Case I*, the focus is on understanding the dispatch strategy impacts on the whole-plant partial load limit and the corresponding impact on the volume of *upward* frequency control services from the 50 MW HE plant. In this case, two main dispatch strategies are investigated, i.e., AVA and DCA, considering three scenarios with different stack partial load limit values: 1) P_{min}= 0 MW, 2) P_{min}= 1 MW, and 3) P_{min}= 2 MW. The HE plant operates at 30 MW before the contingency (P_{set}=30 MW). If the DCA is embedded in the dispatch control unit, six stacks are online and each operates at 5 MW, while the remaining four stacks are off. Under the AVA dispatch strategy, the 30 MW power is equally shared among 10 stacks, thus each stack operating at 3 MW. As shown in Fig. 3(a), a frequency disturbance of 1 Hz is applied to the HE terminals at t = 5 s (Fig. 3(a)). Fig. 3(b) (dashed line) shows how the HE droop controller changes the P_{plant}^{ref} value in response to the frequency drop of 1 Hz.

In the first scenario with P_{min} = 0 MW, both dispatch strategies make an equal 30 MW footroom available for upward frequency response. This is since each stack can reduce its power consumption down to 0 MW. Given the 23 MW/Hz droop gain (Table I), 23 MW frequency response is provided to the external system in the first scenario (Fig. 3(b)).

In the second scenario with P_{min}= 1 MW, however, the footroom provided by the AVA and DCA strategies are 24 MW and 20 MW, respectively. As per Fig. 3(c), the reference power change reference by the droop control is 23 MW. While the DCA-operated plant can achieve this change due to its sufficient footroom, the AVA-operated plant cannot meet the desirable power change due to the available footroom limited to 20 MW.

The third scenario further demonstrates that the desirable frequency response volume, according to the active power-frequency droop characteristic, is even more restricted and may not be achievable when the AVA strategy is applied to the electrolysis plant with a higher stack partial load limit (e.g., P_{min} =2 MW in the third scenario). In this scenario, the footroom provided by the AVA and DCA strategies are 10 MW and 18 MW, respectively. As shown in Fig. 3(d), only 10 MW is provided from the AVA-operated HE plant as a response to the frequency disturbance of 1 Hz, while the DCA-operated plant provides 18 MW frequency response. Differences in the speed of the frequency control response resulting from the mentioned dispatch strategies can also be noted, which will be further discussed in the following case study.

C. Case II: Dispatch Strategy Impacts on the Whole-plant Ramp Rate Limit and the Speed of the HE Frequency Response

The 50 MW scaled-up HE system described in Section III-A is simulated under three different scenarios: 1) No ramp rate limitation considered, 2) the 50 MW plant with R_i = 5 MW/s ramp rate limitation on each stack, and 3) the 50 MW plant with R_i = 2.5 MW/s ramp rate limitation on each 5 MW stack. As shown in Fig. 4(a), a 1 Hz frequency step is applied at t = 5 s. As shown in Fig. 4(b), when there is no ramp rate limit, HE plant increases its power consumption to track the power reference produced by the active power-frequency characteristic. When no ramp rate limitation is imposed, changing the dispatch strategy does not lead to difference in the speed of the HE frequency response.

In the second and third scenarios with ramp rate limitations, however, Fig. 4(c) and Fig. 4(d) demonstrate that per-stack limits of 5 MW/s and 2.5 MW/s lead to different aggregated plant ramp rates and response times for the two dispatch strategies, even though the stacks and their individual R_i values are identical. Under the AVA strategy, all stacks are in operation and thus ramp up simultaneously, so their parallel contributions combine, yielding a whole-plant ramp rate roughly ten times that of a single stack. Under the DCA

979-8-3315-8138-1

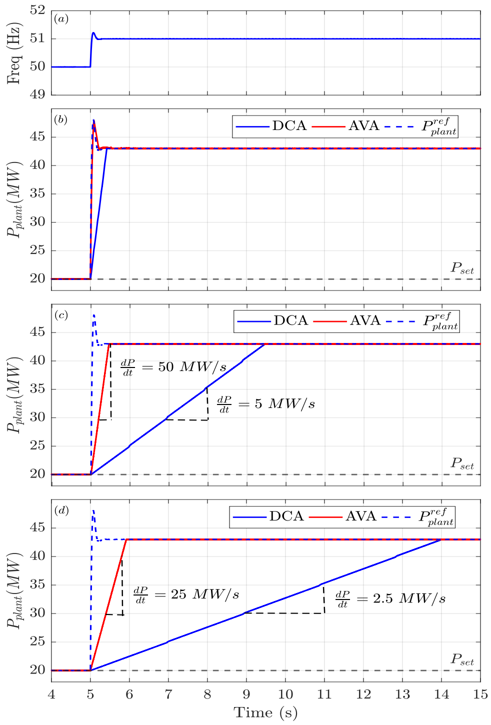

Fig. 4. Case II simulation results: (a) System frequency, (b) Results with no ramp rate limit, (c) Results with a ramp rate value of R_i = 5 MW/s, (d) Results with a ramp rate value of R_i = 2.5 MW/s.

strategy, however, stacks ramp up sequentially, only one stack increases its power at a time, meaning the plant response mirrors the individual stack's ramp rate until the next stack begins frequency response provision.

IV. Conclusion

This paper presented a detailed dynamic model of a scaled-up electrolysis plant consisting of multiple stacks participating in frequency control services. The model incorporates individual stack models, the power-electronic interface, a dispatch control unit, and essential operational constraints including partial load and ramp rate limits. Focusing on the Average Allocation (AVA) and Daisy-Chain Allocation (DCA) strategies, the study examined how the choice of dispatch strategy influences HE frequency response volume and speed.

The simulation results showed that AVA-operated plants with non-zero stack partial load limits experience a reduction in available footroom for upward frequency response. Also, DCA-operated plants exhibit slower frequency response when the HE stacks are subject to non-zero ramp rate limitations. Furthermore, the analysis demonstrated that the aggregate partial load and ramp rate limits of a multi-stack electrolysis plant can differ significantly from the limits of an individual stack, depending on the adopted power dispatch strategy.

These findings underscore the importance of considering scale-up effects and dispatch strategies in service provision from large-scale HEs, which should be considered by system operators and project developers when planning for HE integration into ancillary service markets. Future works will include developing an analytical formulation of scale-up requirements and quantifying their impacts on HE services.

Acknowledgment

CSIRO, Australia's national science agency is enabling Australian researchers to participate in the EPICS Centre with partners in the US and UK as part of the NSF Global Centers program, supported by the Science and Industry Endowment Fund.

References

[1] M. G. Dozein, A. Jalali, and P. Mancarella, "Fast frequency response from utility-scale hydrogen electrolyzers," *IEEE Transactions on Sustainable Energy*, vol. 12, no. 3, pp. 1707–1717, 2021.

[2] Department of Climate Change, Energy, the Environment and Water, "Growing Australia's hydrogen industry," Online, accessed: Nov. 11, 2025. [Online]. Available: https://www.dcceew.gov.au/energy/hydrogen

[3] S. D. Tavakoli *et al.*, "Grid-forming services from hydrogen electrolyzers," *IEEE Trans. on Sustainable Energy*, vol. 14, no. 4, pp. 2205–2219, 2023.

[4] H. Biabani, A. Aminlou, M. M. Hayati, H. Majidi Gharehnaz, and M. Abapour, *Green Hydrogen Research and Development Projects in the European Union*, 03 2024, pp. 301–320.

[5] UK Government, Department for Business, Energy Industrial Strategy (BEIS), "Gigastack Phase 2: Pioneering UK Renewable Hydrogen," Department for Business, Energy Industrial Strategy, London, UK, Public Report, 2021.

[6] New Energy and Industrial Technology Development Organization (NEDO), "Fukushima Hydrogen Energy Research Field (FH2R)," NEDO, Tokyo, Japan, Tech. Rep., 2020.

[7] H. Lange, A. Klose, L. Beisswenger, D. Erdmann, and L. Urbas, "Modularization approach for large-scale electrolysis systems: a review," *Sustainable Energy & Fuels*, vol. 8, 2024.

[8] M. G. Dozein, A. M. De Corato, and P. Mancarella, "Virtual inertia response and frequency control ancillary services from hydrogen electrolysers," *IEEE Trans. on Power Systems*, vol. 38, no. 3, pp. 2447–2459, 2023.

[9] M. Agredano-Torres, M. Zhang, L. Söder, and Q. Xu, "Decentralized dynamic power sharing control for frequency regulation using hybrid hydrogen electrolyzer systems," *IEEE Trans. on Sustainable Energy*, vol. 15, no. 3, pp. 1847–1858, 2024.

[10] C. Huang, Y. Zong, S. You, and C. Træholt, "Analytical modeling and control of grid-scale alkaline electrolyzer plant for frequency support in wind-dominated electricity-hydrogen systems," *IEEE Trans. on Sustainable Energy*, vol. 14, no. 1, pp. 217–232, 2023.

[11] A. Guan, S. Zhou, W. Gu, Z. Wu, X. Ai, and J. Fang, "Frequency response coefficient optimal allocation strategy for multi-stacks alkaline water electrolyzer plant," *International Journal of Hydrogen Energy*, vol. 89, pp. 151–160, 2024.

[12] D. Guilbert and G. Vitale, "Improved hydrogen-production-based power management control of a wind turbine conversion system coupled with multistack proton exchange membrane electrolyzers," *Energies*, vol. 13, no. 5, p. 1239, 2020.

[13] X. Lu *et al.*, "Optimization of power allocation for wind-hydrogen system multi-stack PEM water electrolyzer considering degradation conditions," *International Journal of Hydrogen Energy*, vol. 48, no. 15, pp. 5850–5872, 2023.

[14] W. Zheng *et al.*, "Optimization of power allocation for the multi-stack PEMEC system considering energy efficiency and degradation," *International Journal of Hydrogen Energy*, vol. 53, pp. 1210–1225, 2024.

[15] F. Díaz-González, A. Sumper, and O. Gomis-Bellmunt, *Energy Storage in Power Systems*. John Wiley & Sons, 2016.

[16] N. Taranin, M. Ghazavi, O. Saborío-Romano, and N. Cutululis, "On the ramp-rate limitation of electrolysis plants: Modeling fundamentals and system-level impact analysis," *IEEE Trans. on Sustainable Energy*, vol. PP, pp. 1–12, Sep. 2025.

[17] S. H. Meetiyagoda, B. Bahrani, and M. G. Dozein, "Distribution-connected electrolyzers with partial loading limit and power response characteristics," in *2025 IEEE Kiel PowerTech*, 2025, pp. 1–7.

979-8-3315-8138-1